Comparison of Discretization Methods for Device Simulation

Daniel J. Cummings, Mark E. Law
Department of Electrical and Computer Engineering
University of Florida
Gainesville, FL, USA
E-mail: danieljc@ufl.edu

Steve Cea[1], Tom Linton[2]
Intel Corporation
[1]Hillsboro, OR, USA
[2]Santa Clara, CA, USA

***Abstract*—The characteristics of semiconductor devices are modeled by three coupled nonlinear partial differential equations consisting of the electron continuity, hole continuity, and Poisson equations. A variety of discretization approaches can be used to solve these equations. This paper compares finite volume Scharfetter-Gummel and finite element quasi-Fermi discretization schemes for a variety of devices and mesh element types. The simulation results show that a quasi-Fermi approach may be preferable to the more common finite volume Scharfetter-Gummel method for certain device simulation applications.**

Keywords-device simulation; discretization methods; finite volume method; finite element method; single-event upset

I. INTRODUCTION

Three coupled nonlinear partial differential equations form the foundation of modern semiconductor device modeling. These equations, consisting of the Poisson, electron continuity and hole continuity equations, can be solved using a variety of approaches [1]. Current device simulators typically use a finite volume Scharfetter-Gummel (FVSG) discretization scheme to solve the equations by using electron, hole, and electrostatic potential variables (n, p, ψ) [2]. This study compares the FVSG method to a less prevalent finite element quasi-Fermi (FEQF) approach which solves the equations in terms of electron and hole quasi-Fermi levels and electrostatic potential (ϕ_n, ϕ_p, ψ) [3,4].

One area where it may be profitable to investigate both methods is the simulation of radiation effects on semiconductor devices. Ideally, in a FVSG scheme, the grid should be aligned in the direction of current flow, since current flow is defined based on the grid edges. However, for radiation events, particle strikes can generate carriers throughout the device and the resulting carrier action is rarely aligned with the grid. For these non-ideal conditions the FEQF method could be more accurate and stable than the FVSG approach, since current flow in the FEQF method is not defined on the edges.

The remainder of this paper is organized as follows: after a brief discussion of the simulation tool, the discretization methods will be presented in detail. Next, the grid element types and the physical models implemented in the simulation tool will be defined. Simulation results from a MOSFET device are used to show that both discretization methods give comparable results. Finally, a particle strike simulation will be used to evaluate the benefits of the FEQF approach as compared to the FVSG method.

II. SIMULATION METHOD AND PHYSICAL MODELS

A. Simulation Tool

The Florida Object Oriented Device Simulator (FLOODS), using the drift-diffusion transport model, was used to simulate the FVSG and FEQF discretization methods. FLOODS supports a variety of mesh element types for 2-D and 3-D simulations which are used for comparison in addition to the FVSG and FEQF schemes. The simulation tool uses the UMFPACK direct linear solver [5].

B. Discretization

The set of coupled, time-dependent partial differential equations that govern semiconductor device behavior can be written as

$$\nabla \cdot (\varepsilon \nabla \psi) = -q\left(p - n + N_D^+ - N_A^-\right) \tag{1}$$

$$\frac{dn}{dt} = \frac{1}{q}\nabla \cdot J_n - U_n \tag{2}$$

$$\frac{dp}{dt} = -\frac{1}{q}\nabla \cdot J_p - U_p \tag{3}$$

where ε is the dielectric permittivity, q the elementary charge, ψ is electrostatic potential, n and p are the electron and hole densities, N_D^+ and N_A^- are the ionized donor and acceptor densities, J_n and J_p are the electron and hole current densities, and U_p, U_n are the net electron and hole recombination rates.

To obtain a closed system of equations, the current densities are written as quasi linear functions of driving potential in gradient form

$$J_n = -q\mu_n n \nabla \phi_n \tag{4}$$

$$J_p = -q\mu_p p \nabla \phi_p \tag{5}$$

where ϕ_n, ϕ_p are the quasi-Fermi levels and μ_n, μ_p are the mobilities. The quasi-Fermi levels are functions of the electrostatic potential and the electron and hole carrier densities. For example, in the case of a nondegenerate

semiconductor, the quasi-Fermi levels can be written using Boltzmann's relations as

$$\phi_n = \psi - \frac{kT}{q}\ln(n/n_i) \quad (6)$$

$$\phi_p = \psi + \frac{kT}{q}\ln(p/n_i) \quad (7)$$

where kT/q is the thermal voltage and n_i is the intrinsic carrier concentration. Using these relations, the current density in (4) and (5) can be written in the familiar relationship as the sum of drift and diffusion components

$$J_n = qn\mu_n \mathrm{E} + qD_n \nabla n \quad (8)$$

$$J_p = qp\mu_p \mathrm{E} - qD_p \nabla p \ . \quad (9)$$

where E is the electric field and $D_{n,p}$ is the Einstein relation.

When using electron and hole densities as solution variables in a finite volume scheme, each partial differential equation is integrated over a control volume *A* surrounding each node. The control volume is defined by the perpendicular bisectors of the mesh element sides. The divergence operators are integrated using Green's formula so that the continuity equation can be discretized and the current $J_{n,p}$ can be evaluated using the Scharfetter-Gummel formula [2].

For the finite element quasi-Fermi scheme, the continuity equations can be rewritten in terms of (4) and (5) and the gradient of $\phi_{n,p}$ can be computed over each mesh element. In FLOODS, the discretization for the finite element method starts by separating the domain into smaller subspaces (e.g. triangles or rectangles). Then, the subspaces are discretized into a set of points on which piecewise linear polynomial interpolation is used. In summary, this method is a process for producing an optimal piecewise interpolant to the true solution. Finite element methods are discussed in much greater detail in [6].

C. Element Types

Since discretization methods are dependent on the geometry of the mesh, a variety of meshes composed of different element types were used for 2-D and 3-D simulations. For 2-D simulations, quad, quad-diagonal, and randomized triangular meshing schemes were used (Fig.1). For the generation of 3-D meshes, tetrahedron and hexahedron (brick) element types were used.

D. Physical Models

A variety of physical models are implemented in the simulation tool. For mobility, the simulation models used are the Philips mobility, Lombardi mobility, and velocity saturation models. The Philips unified mobility model unifies the description of majority and minority carrier bulk mobilities and takes into account carrier-carrier scattering, screening of ionized impurities, and clustering of impurities [7]. The Lombardi model is a function of surface acoustic phonon scattering and surface roughness scattering [8]. For recombination-generation the Shockley-Read-Hall (SRH) and Auger band-to-band models were used. The physical models were divided into two sets for the simulations so that the discretization methods could be tested under different circumstances (Table 1). In addition, this comparison will show the impact of electric field dependent models such as Lombardi mobility and velocity saturation.

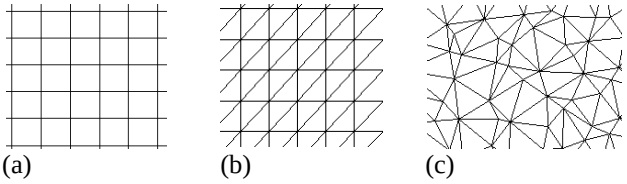

Figure 1. 2-D Mesh Types. (a) Rectangular or Quad, (b) Quad-diagonal (c) Randomized Triangle

TABLE I. PHYSICAL MODEL SETS

Model Set	Physical Models
Simple	Constant Mobility ($\mu_{n,p}$ = 150 cm^2/V·s)
Advanced	Philips Mobility, Lombardi Mobility, Velocity Saturation, SRH & Auger Recombination

III. TEST CASES AND RESULTS

Both FVSG and FEQF methods were compared for a variety of mesh element types and device structures. Additionally, the x-, y-, z-axis grid spacings were varied since smaller spacings give a more accurate result but require more computation time. The assembly time, linear solve time, and number of Newton iteration steps were measured for each simulation.

A. Short-Channel MOSFET Simulations

For a baseline comparison, a common MOSFET device was simulated to compare the FVSG and FEQF methods. A simple short-channel nMOSFET device with a 40nm gate and Gaussian doping profiles in the source/drain was created as a template.

For 2-D nMOS simulations, the FVSG and FEQF methods performed very similarly in terms of output current and number of Newton steps required for convergence. For rectangular and quad-diagonal mesh elements, both methods gave similar nMOS I_{ON} currents at very tight grid spacings (Fig. 2). The

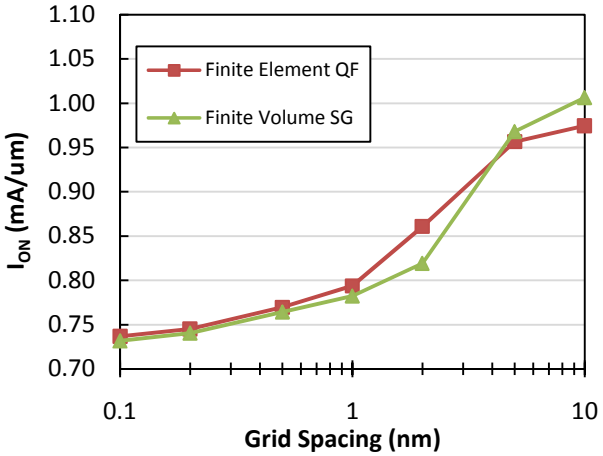

Figure 2. nMOS I_{ON} currents using the advanced physical model set for a variety of grid spacings

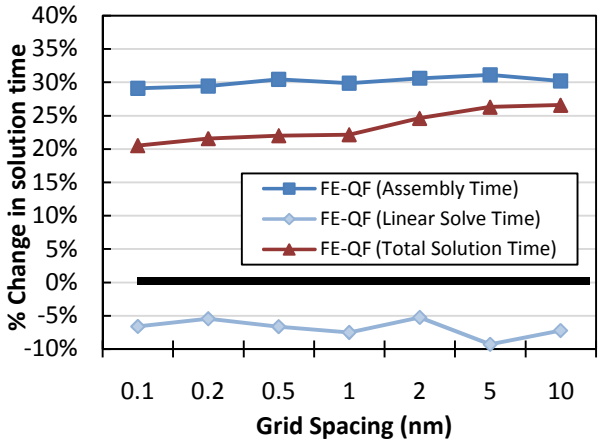

Figure 3. Percent change in solution time per Newton step for the FEQF when compared to the FVSG (black baseline). Based on the nMOS template with quad-diagonal elements and advanced physical models.

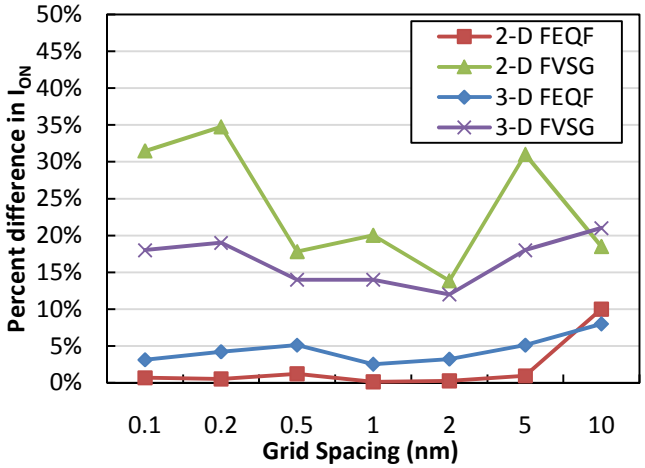

Figure 4. The FVSG method loses accuracy for highly non-Delaunay mesh conditions in the nMOS channel. The FEQF method is less affected by the non-ideal mesh conditions. Average based on 10 simulations per grid spacing.

currents began to vary as the grid spacings increased above 1 nm, though both methods followed a similar trend. The assembly time for the FEQF approach was longer than the FVSG, and on average resulted in a ~22% increase in total solution time per Newton step (Fig. 3). The time increase is due to the fact that in the FVSG method, each edge is assembled once whereas for the FEQF method assembly is done element by element. Thus for the FEQF scheme, each edge is effectively assembled twice. The results from the advanced and simple model sets followed same assembly time trend.

An interesting difference between methods occurred when the mesh element nodes were displaced as a test of non-ideal mesh conditions. With the exception of the gate oxide channel interface and outside boundaries, each node inside the nMOS was randomly displaced by up to 40% of the initial grid spacing. The randomization of the grid created a large number of negative edge couplings which implies non-Delaunay mesh elements throughout the structure. The negative coupling values were not zeroed out. For 2-D, the non-Delaunay conditions were created by randomizing quad-diagonal nodes. Non-Delaunay conditions in 3-D simulations were created using tetrahedron element types. Using the default nMOS structure (normal ideal grid) as a baseline, the results for both FEQF and FVSG methods were compared against equivalent structures with randomly displaced nodes. For both 2-D and 3-D simulations, the FEQF method performed very accurately in terms of I_{ON} for both normal and randomized grids (Fig. 4). However, the I_{ON} results for the FVSG method deviated by a large amount, especially at small grid spacings. As the node randomization was reduced, the FVSG method increased in accuracy.

When using the FVSG method, solution convergence was a problem for the 3-D nMOS device simulations if non-Delaunay elements were predominant. For both tetrahedra and bricks, if the mesh elements under the MOS gate were too flat (> 5:1 width:depth ratio) the FVSG solution would not converge. The FEQF method did not have trouble converging with this ratio.

B. Charge Collection Simulations

The simulation of ionizing-radiation-induced charge collection and single-event upset (SEU) is a growing area of device simulation since sensitivity to SEU is expected to increase for both in memories and core logic. By extrapolating scaling effects, some studies predict an increase in soft error susceptibility of ~40% per technology generation [9].

A reversed biased pn diode was used as a good representation of the source/drain junctions that are responsible for charge collection in MOSFETs. A charge collection simulation was performed in 3-D since in 2-D, all quantities are assumed to be extruded into the third dimension which leads to a misrepresentation of the charge density. A 3-D pn diode was created as a template and tested with both tetrahedra and brick elements. A charge cloud was generated into the depth of the device to model the electron-hole pairs that are generated during a particle strike.

Both methods converged well for DC bias conditions. However, the simulation results show that the FEQF method converged more reliably in the transient domain than the FVSG method for different mesh spacings and charge concentrations. This could imply that the FEQF scheme handles isotropic current flow with more stability. This explanation is substantiated by the numerical stability problems that have been observed in the past for 3-D FVSG charge collection simulations [10]. In terms of mesh element types, both the FVSG and FEQF methods converged better for bricks than for tetrahedra, especially at high charge concentrations.

Another major difference between discretization methods was noticed in their transient simulation times. The FVSG required more Newton steps for every solution time step than the FEQF method. Even though the assembly time for the FEQF method is ~22% longer, the total simulation time, on average, for a charge collection transient was less than that of the FVSG method (Fig. 5). Because detailed charge collection

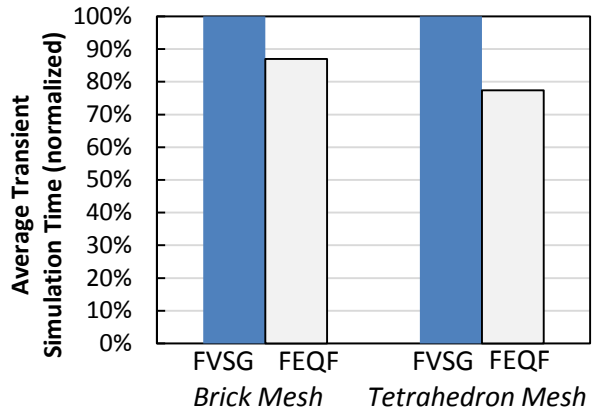

Figure 5. Normalized average total transient simulation time. The average was taken over 15 simulations each with difference charge concentrations.

simulations in 3-D often take a day or more to complete, this time savings could be quite significant.

IV. Conclusion

For the short channel nMOS simulations, both the FVSG and FEQF methods gave agreeing I_{ON} results over a variety of grid spacings and element types. However, for a MOSFET grid with a non-ideal mesh (non-Delaunay elements), the FVSG method is prone to inaccuracy suggesting a high sensitivity to mesh alignment at channel interfaces. Based on these results, the FEQF approach would most likely provide more accurate results for rough or curved interfaces or situations where meshing is non-ideal. However, the FEQF method has the disadvantage of a longer DC simulation time due to a longer assembly time. For 3-D charge collection simulations, the FEQF method outperformed the FVSG approach due to a higher convergence rate which may be due to a better handling of isotropic current flow. The total transient simulation time was also less for the FEQF method.

Even though the FVSG method is by far the most accepted discretization scheme in practice today, the simulation results presented in this paper indicate that the finite element quasi-Fermi discretization approach is a viable and in some cases preferable alternative which should not be overlooked. Building on these results, future avenues of study could include other previously suggested discretization schemes such as Slotboom variable or log(n, p) variable based approaches [11].

References

[1] C.S. Rafferty, M. R. Pinto, and R. W. Dutton, “Iterative Methods in Semiconductor Device Simulation,” IEEE Trans. Computer-Aided Design, vol. CAD-4, pp. 462-471, October 1985.

[2] D. Scharfetter and H. K. Gummel, “Large-signal analysis of a silicon Read diode oscillator,” IEEE Trans. Electron Devices, vol. 16, pp. 64-77, 1969.

[3] J. Machek and S. Selberherr, “A Novel Finite-Element Approach to Device Modeling,” IEEE Trans. Electron Devices, vol. 30, pp. 1083-1092, September 1983.

[4] S. Micheletti, “Stabilized finite elements for semiconductor device simulation,” Comput & Visual Sci., vol. 3, pp. 177-183, 2001.

[5] T.A. Davis, ”Algorithm 832: UMFPACK, an unsymmetric-pattern multifrontal method,” ACM Trans. on Mathematical Software, vol. 30, pp. 196-199, June 2004.

[6] O. C. Zienkiewicz and R. L. Taylor, The Finite Element Method. 4th Ed., McGraw-Hill, London, 1991.

[7] D. B. M. Klaassen, “A Unified Mobility Model for Device Simulation-I. Model Equations and Concentration Dependence,” Solid-State Electronics, vol. 35, pp. 953–959, 1992.

[8] M. N. Darwish et al., “An Improved Electron and Hole Mobility Model for General Purpose Device Simulation,” IEEE Transactions on Electron Devices, vol. 44, no. 9, pp. 1529–1538, 1997.

[9] P. E. Dodd, L. W. Massengill, "Basic mechanisms and modeling of single-event upset in digital microelectronics," IEEE Trans. on Nuclear Science, vol.50, pp. 583-602, June 2003.

[10] P. E. Dodd, “Device simulation of charge collection and single-event upset,” IEEE Trans. on Nuclear Science, vol. 43, pp. 561-575, April 1996.

[11] M. R. Pinto, Comprehensive Semiconductor Device Simulation for VLSI, Ph.D. Thesis, Stanford University, August 1990.